

## 20 Years of ClO Measurements in the Antarctic Lower Stratosphere

Gerald E. Nedoluha<sup>1</sup>, Brian J. Connor<sup>2</sup>, Thomas Mooney<sup>2</sup>, James W. Barrett<sup>3</sup>, Alan Parrish<sup>4</sup>, R. Michael Gomez<sup>1</sup>, Ian Boyd<sup>2</sup>, Douglas R. Allen<sup>1</sup>, Michael Kotkamp<sup>5</sup>, Stefanie Kremser<sup>6</sup>, Terry Deshler<sup>7</sup>, Paul Newman<sup>8</sup>, and Michelle L. Santee<sup>9</sup>

<sup>1</sup>Naval Research Laboratory, Washington, D. C., USA

<sup>2</sup>BC Scientific Consulting LLC, Stony Brook, NY, USA

<sup>3</sup>Stony Brook University, Stony Brook, New York, USA

<sup>4</sup>Department of Astronomy, University of Massachusetts, Amherst, MA, USA

10 <sup>5</sup>National Institute of Water and Atmospheric Research, Lauder, New Zealand

<sup>6</sup>Bodeker Scientific, Alexandra, New Zealand

<sup>7</sup>Department of Atmospheric Science, University of Wyoming, Laramie, WY, USA

<sup>8</sup>NASA Goddard Space Flight Center, Greenbelt, MD, USA

<sup>9</sup>Jet Propulsion Laboratory, California Institute of Technology, Pasadena, California, USA

15 *Correspondence to:* Gerald E. Nedoluha (nedoluha@nrl.navy.mil)

**Abstract.** We present 20 years (1996-2015) of austral springtime measurements of chlorine monoxide (ClO) over Antarctica from the Chlorine Oxide Experiment (ChlOE1) ground-based millimeter wave spectrometer at Scott Base, Antarctica, as well 12 years (2004-2015) of ClO measurements from the Aura Microwave Limb Sounder (MLS). From August onwards we observe a strong increase in lower stratospheric ClO, with a peak column amount usually occurring in early September. From mid-September onwards we observe a strong decrease in ClO. In order to study interannual differences, we focus on a 3-week period from August 28 to September 17 for each year, and compare the average column ClO anomalies. These column ClO anomalies are shown to be highly correlated with the average ozone mass deficit for September and October of each year. We also show that anomalies in column ClO are strongly anti-correlated with 30 hPa temperature anomalies, both on a daily and an interannual timescale. Making use of this anti-correlation we calculate the linear dependence of the interannual variations in column ClO on interannual variations in temperature. By making use of this relationship, we can better estimate the underlying trend in the total chlorine ( $Cl_y = HCl + ClONO_2 + HOCl + 2 \times Cl_2 + 2 \times Cl_2O_2 + ClO + Cl$ ). The resultant trends in  $Cl_y$ , which determine the long-term trend in ClO, are estimated to be  $-0.5 \pm 0.2\% \text{ yr}^{-1}$ ,  $-1.4 \pm 0.9\% \text{ yr}^{-1}$ , and  $-0.6 \pm 0.4\%$

20  
25  
30

yr<sup>-1</sup>, for zonal MLS, Scott Base MLS (both 2004-2015), and ChIOE (1996-2015) respectively. These trends are within 1σ of trends in stratospheric Cl<sub>y</sub> previously found at other latitudes. The decrease in ClO is consistent with the trend expected from regulations enacted under the Montreal Protocol.

5

## 1. Introduction

Chlorine monoxide (ClO) is central to the formation of the Antarctic ozone hole. It is both the direct product of the reaction between chlorine (Cl) and ozone (O<sub>3</sub>) and the catalytic agent in the most important ozone-depleting chemical cycle ( $\text{Cl} + \text{O}_3 \rightarrow \text{ClO} + \text{O}_2$ ;  $\text{ClO} + \text{O} \rightarrow$   
10  $\text{Cl} + \text{O}_2$ ; Waters et al., 1993, Salawitch et al., 1993). Understanding trends in ClO is therefore critical to our understanding of polar ozone recovery. The Antarctic spring is unusual in that, in the lower stratosphere, most of the available total chlorine (Cl<sub>y</sub>) is present in its reactive forms (ClO<sub>x</sub> = ClO + 2xCl<sub>2</sub>O<sub>2</sub>). The amount of ClO in the Antarctic vortex is dependent upon both the available Cl<sub>y</sub> and on the prevalence of polar stratospheric clouds (PSCs), which provide the  
15 surfaces for heterogeneous processes that convert unreactive chlorine species into ClO<sub>x</sub>. While Cl<sub>y</sub> will vary from year-to-year due to dynamical effects (Strahan et al., 2014), it will vary much more slowly than ClO, which, because of its sensitivity to the prevalence of PSCs, is very sensitive to interannual variations in temperature. The primary goal of this study is to estimate the trend in Cl<sub>y</sub> in the Antarctic lower stratosphere, during the annual formation of the ozone  
20 hole, over the period 1996 to 2015.

The ClO molecule has emission lines at microwave frequencies, and the first ground-based measurements of stratospheric ClO were made using a microwave radiometer in 1980 (Parrish et al., 1981). High concentrations of ClO in the lower stratosphere over Antarctica were first measured using this technique in 1986 (de Zafra et al., 1987; Solomon et al., 1987). The  
25 Chlorine Oxide Experiment (ChIOE1) ground-based millimeter wave spectrometer was permanently deployed at Scott Base, Antarctica (77.85° S, 166.77° E), by Stony Brook University and the National Institute of Water and Atmospheric Research (NIWA) in February 1996. Details of the measurement technique, data analysis, and error analysis were presented in Solomon et al. (2000). ChIOE1 is currently jointly operated by the Naval Research Laboratory  
30 (NRL) and NIWA. Both this instrument and the ChIOE3 instrument, which operated at Mauna

Kea, Hawaii, until 2015, are part of the Network for the Detection of Atmospheric Composition Change (NDACC). A new ChlOE4 instrument has now been deployed at Mauna Loa, Hawaii.

In this paper, we describe the measurement technique and present results from the ChlOE1 time series from 1996-2015. Measurements are only shown from mid-August to mid-  
5 October, when ClO daytime mixing ratios can reach up to  $\sim 2$  ppbv. We show, from 2004 onwards, ClO measurements from the Aura Microwave Limb Sounder (MLS), both coincident with Scott Base and zonally averaged at the latitude of Scott Base. The ChlOE1 measurements were previously compared with the v1.5 MLS retrievals for the austral spring of 2005 (Connor et al., 2007). Comparisons of measurements taken within  $\pm 30$  minutes of the MLS ascending orbit  
10 overpass showed agreement of  $11 \pm 8\%$  in the peak mixing ratios.

We also show annual anomalies for measurements during the 3 weeks when the stratospheric ClO column densities generally reach their maximum values, and compare these anomalies with interannual anomalies in temperature, as provided by the Modern Era Reanalysis for Research and Applications (MERRA) (Rienecker et al., 2011). We use the 20 years of  
15 ChlOE measurements and 12 years of MLS measurements to derive a relationship between the interannual anomalies in ClO column and those in 30 hPa temperature. We then make use of this relationship to derive an estimate of  $Cl_y$  trends in the Antarctic vortex.

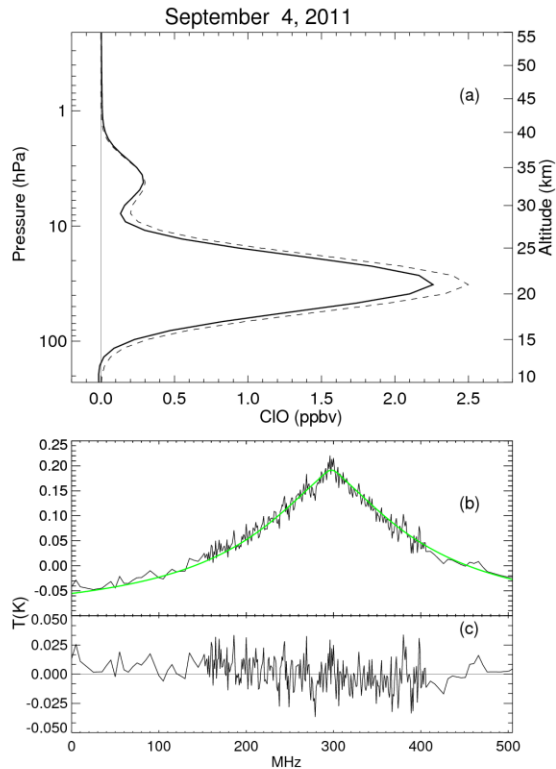
## 2. ClO Measurements

The ChlOE ground-based radiometer measures the thermally excited rotational emission  
20 lines near 278.63 GHz. The spectrometer bandwidth permits measurement of the pressure-broadened lineshape from which ClO altitude profiles are retrieved. The instrument is a cryogenically cooled ( $\sim 20$  K) heterodyne receiver, tuned to observe the ClO transition by adjustment of a phase-locked local oscillator. It is coupled to a spectrometer with 506 MHz total  
25 bandwidth, which is approximately the width of the ClO line at 15 km altitude.

At night, the ClO emission is much weaker and narrower, because nearly all ClO in the lower stratosphere rapidly converts to chlorine peroxide ( $Cl_2O_2$ ) after sunset (Solomon et al., 2002). This allows us, in the ground-based measurements, to remove the instrumental baseline and a small number of interfering atmospheric spectral lines in the instrument bandpass  
30 (primarily the ozone line at 278.521 GHz) by subtracting the nighttime spectrum from the daytime one. For these measurements we have defined day as the period from 3 hours after

sunrise to 1 hour before sunset, and night as the period from 4 hours after sunset to 1 hour before sunrise. Sunrise and sunset are defined to occur when the solar zenith angle is  $94.5^\circ$  at the surface (equivalent to  $90^\circ$  near  $\sim 20$  km altitude). These day and night variations were chosen empirically, in an attempt to estimate daytime and nighttime equilibrium concentrations of ClO, by excluding times near sunrise and sunset when we observed rapid diurnal changes in ClO. If more observations are included in either daytime or nighttime integrations, these periods of rapid change are partially included, significantly changing the mean values. If fewer observations are included, the integrated spectra are noisier and the mean ClO is correspondingly more uncertain.

A retrieval of the “day minus night” spectrum, and thus of the day ClO mixing ratio less the night mixing ratio, is performed by a three-stage process, described in detail by Solomon et al. (2000). The first stage determines the altitude of the peak of the lower stratospheric distribution as a function of date, by performing retrievals on a full season of data, using an a priori profile without a separate lower stratospheric component. In the second stage, the a priori ClO distribution consists of a climatological profile having a peak in the lower stratosphere determined by stage 1 at  $\sim 30$  hPa (22 km) in mid-August to  $\sim 48$  hPa (19 km) by late September, with a secondary peak in the upper stratosphere at  $\sim 5$  hPa. The second-stage retrieval is simply a nonlinear least-squares-fit of a single multiplier applied to the lower stratospheric distribution. The climatological distribution, modified by the retrieved multiplier, is used as the a priori distribution for the third stage, which is a maximum a posteriori solution as given by Rodgers (2000, e.g., equation (4.5)). Figure 1 shows a ChLOE1 day minus night retrieval for September 4, 2011. The retrieved and a priori profiles both have two mixing ratio peaks, one peak in the upper stratosphere and a much larger peak in the lower stratosphere. The lower stratospheric peak is only present when inactive chlorine is converted to active chlorine on the surface of PSCs, and is therefore only observed under the extremely cold Arctic and Antarctic conditions where PSC formation is possible (temperatures below  $\sim 195$  K). The upper stratospheric ClO peak can be observed at any location, but because of the weak signal, the best ground-based measurements require extended integrations ( $\sim 1$  week) from a high-altitude site. Measurements of this ClO peak, as made from the ChLOE3 instrument at Mauna Kea, have been shown in Nedoluha et al. (2011) and Connor et al. (2013). Since all of the measurements shown here are from the ChLOE1 instrument, we will henceforth refer to this instrument simply as ChLOE.



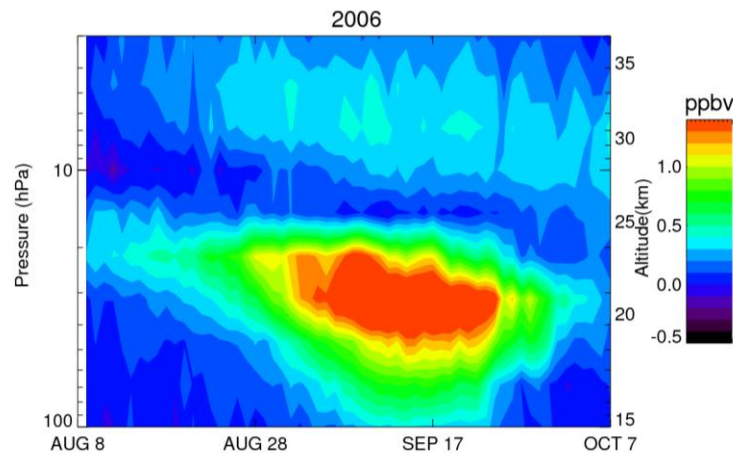
5 **Figure 1 –a:** The retrieved day minus night CIO mixing ratio profile for September 4, 2011 (solid line), and the a priori profile for that day (dashed line), as a function of pressure (left y-axis) and geometric altitude (right y-axis) . **b:** The measured (black line) and modeled (green line) spectra. **c:** The measured minus modelled residual spectrum.

As is clear in Figure 1, and has previously been shown by ground-based microwave (de Zafra et al., 1987; Solomon et al., 1987, 2000) and satellite measurements (e.g., Waters et al., 1993, Santee et al. 2005), CIO in the Antarctic spring is overwhelmingly concentrated in the lower stratosphere. We shall, throughout this study, make use of the column CIO at altitudes  
 10 above 100 hPa. Any variations in this CIO column during the polar PSC season are dominated by changes in the lower stratospheric peak of CIO.

Aura MLS measurements of CIO are available since 2004. The version 2.2 CIO measurements were validated in Santee et al. (2008). Here, we use the v4.2 retrievals (Livesey et al., 2015). The Aura measurement overpasses near the latitude of Scott Base occur at ~1630 and  
 15 ~2300 LST. The times for these measurements remain consistent within  $\pm 4$  minutes throughout the entire Aura mission. Although it is not possible to replicate the ChIOE diurnal sampling with the twice daily MLS overpass sampling, we shall nevertheless in this study show exclusively MLS daytime (~1630 LST) minus nighttime (~2300 LST) measurements. We note that at the

78°S latitude of Scott Base the sun actually sets before 1630 at 23 km (i.e., near the ClO peak) until August 24.

The typical seasonal evolution of ClO, as measured by MLS, is shown in Figure 2. This figure shows zonal average day minus night MLS measurements within  $\pm 2^\circ$  latitude of Scott Base for 2006. As in Figure 1 both the upper and lower stratospheric peaks in ClO are apparent. The ClO begins to increase in the sunlit portions of the vortex in late May/early June as the reservoir gases, hydrogen chloride (HCl) and chlorine nitrate (ClONO<sub>2</sub>), are converted to ClO. The lower-altitude ClO continues to show a gradual increase until mid-September, and then experiences a sharp decline, as it converts back to the reservoir gases. Santee et al. (2008) present a detailed study of the seasonal evolution of the partitioning between ClO, HCl (from MLS), and ClONO<sub>2</sub> (from the Atmospheric Chemistry Experiment Fourier Transform Spectrometer; ACE-FTS) in the Arctic and Antarctic.



15 **Figure 2 – The zonally averaged daily ClO mixing ratio (day minus night) as measured by Aura MLS for 2006.**

Figure 3 shows measurements of day minus night ClO column from ChLOE during 2006 together with those from the coincident (within  $\pm 2^\circ$  latitude and  $\pm 15^\circ$  longitude of Scott Base) MLS measurements. ChLOE measurements are missing for some days because poor tropospheric weather made it impossible to obtain both the daytime and nighttime spectra required for the retrieval, but the general temporal development is clear in both the MLS and ChLOE datasets. Essentially there is an increase in August, a maximum in mid-September, and then a rapid decrease at the end of winter.

In addition to the daily measurements for 2006, we also plot the ChIOE and MLS climatologies for these datasets. The ChIOE climatology is calculated from the daily average of all measurements taken from 1996-2015, while the MLS climatology is derived from measurements taken from 2004-2015. Calculating the ChIOE climatology using only measurements from 2004-2015 makes very little difference in the analysis. In both cases a 5-day smoothing has been applied. Both datasets show values of the 2006 CIO column that, at least until mid-September, are generally higher than their climatologies. Santee et al. (2011) previously noted that the 2006 Antarctic winter showed strong and prolonged chlorine activation in the lowermost vortex, and postulated that this was the cause of unusually low column ozone that year.

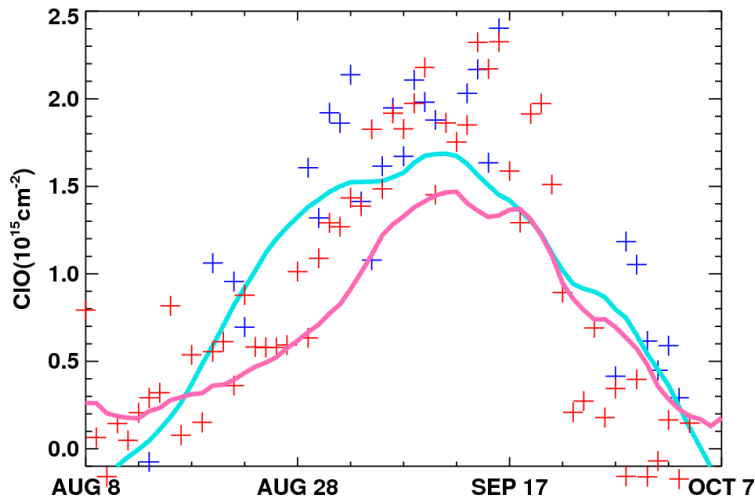
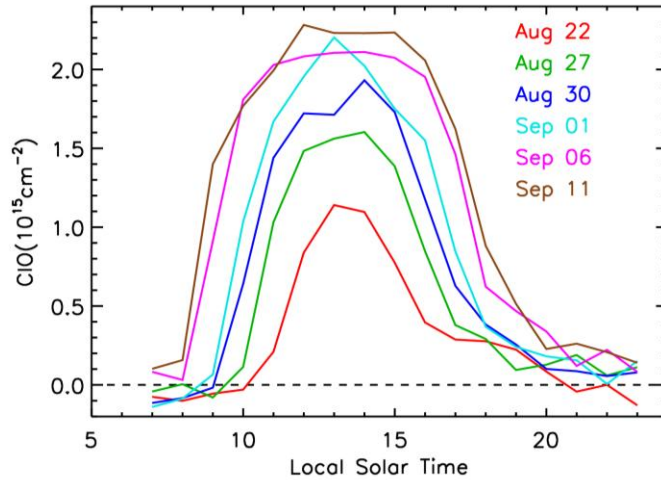


Figure 3 – Daily (day minus night) column density of CIO measurements at altitudes above 100 hPa for mid-August to mid-October 2006 from ChIOE measurements at Scott Base (blue crosses) and from MLS measurements within  $\pm 2^\circ$  latitude and  $\pm 15^\circ$  longitude of Scott Base (red crosses). Also shown are climatologies for this period based on the ChIOE measurements from 1996-2015 (light blue line) and MLS measurements from 2004-2015 (pink line).

Figure 3 shows a clear difference in the seasonal development of the day minus night MLS and ChIOE climatologies. Since the MLS measurements in the vicinity of Scott Base only begin to see sunlit air near the altitude of the CIO peak near August 24, the fast increase in CIO measured by MLS between August 28 and September 7 is to some extent caused by the very large fractional increase in sunlight exposure during this period. Figure 4 shows the diurnal variation of ChIOE CIO column density for measurements at Scott Base on days when hourly measurements were possible. As is seen in the climatologies in Figure 3, the difference between

the MLS and ChIOE measurements decreases as the length of daylight increases and the 1630 LST MLS measurement becomes more representative of a mid-day measurement.



5 **Figure 4 – The diurnal variation of CIO column density at altitudes above 100 hPa at Scott Base as measured from a series of measurement days in 2005. The date given for each curve is the middle date of a 3-day average of hourly measurements.**

We note that Upper Atmosphere Research Satellite (UARS) MLS CIO measurements are available for the years 1991-1993. Using the ground-based ChIOE measurements from Mauna  
 10 Kea, we previously showed that the UARS MLS CIO measurements in the upper stratosphere were consistent with the Aura MLS CIO measurements (agreeing to within  $\sim 1 \pm 4\% (2\sigma)$ ; Nedoluha et al., 2011). However, unlike Aura MLS, UARS MLS was in a precessing orbit, and therefore the local solar times of measurements varied from day to day. Given the large diurnal  
 15 variability of lower stratospheric CIO in the vortex we would require an extremely accurate model in order to be able to usefully compare the UARS MLS CIO measurements with other measurements in this study.

### 3. Annual CIO Anomalies

On the basis of 20 years of springtime lower stratospheric CIO measurements from Scott  
 20 Base, and 12 years of MLS measurement near this latitude, we will provide an estimate of the trend in  $Cl_y$  in this region which underlies the trend in CIO. To calculate this trend, we need a period over which we have an adequate number of elevated CIO measurements, and during which the year-to-year differences resulting from meteorological variations are minimized. As was shown in Figures 2 and 3, there is a gradual increase in CIO at the latitude of Scott Base



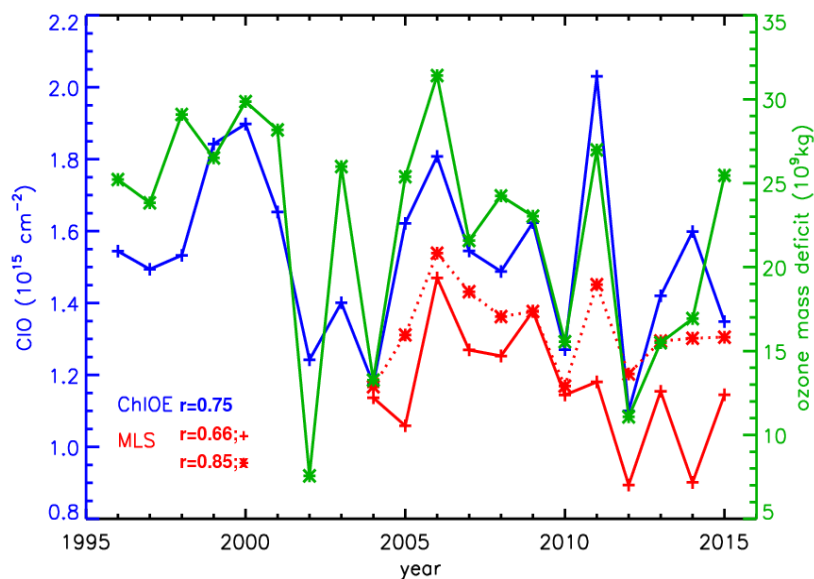
from ~August 28 to September 17. At the latitude of Scott Base (77.85°S), we do not expect that during these dates any of the measurements have occurred outside of the vortex (except possibly in 2002, when the Antarctic stratosphere exhibited an unusual major warming). In the weeks after September 17, there is generally a very sharp drop in ClO, with the exact timing of this drop differing from year to year. As a measure of this increased variation, we note that the standard deviation of the 12 years of MLS measurements near Scott Base increases from 29% of the ClO column on September 17 to 58% of the ClO column on September 22. We therefore choose September 17 as the final day of the period for which we will compare interannual variations. On August 28, the climatological ClO from the ChlOE measurements is similar to that on September 17, and the ChlOE measurements show a steep increase up to this date. The choice of August 28 as the first day for the comparisons provides us a 3-week period with an average of 16.4 daily measurements from ChlOE for each year.

We calculate, for the chosen 3-week period, an annual anomaly for each measurement dataset by taking the average difference from the climatology. We then add back the climatological average column ClO for the period so that we can express changes in ClO both in absolute and in fractional terms. So for each year we plot in Figure 5

$$Y(\text{year}) = Y_{\text{climo}} + [1/n(\text{year})] \Sigma [D(\text{year},\text{day}) - D_{\text{climo}}(\text{day})] \quad (1)$$

where  $Y_{\text{climo}}$  is the dataset-specific climatological average column ClO for the 3-week period,  $n(\text{year})$  is the number of measurements during that period for a specific year,  $D(\text{year},\text{day})$  is the measured column ClO for that day, and  $D_{\text{climo}}(\text{day})$  is the dataset-specific climatological average column ClO for that day of the year. MLS values are shown both for the zonal average (within 77.85°S±2°) and with a further restriction to within ±15° longitude of Scott Base. As expected from the difference in diurnal sampling, the MLS average column day minus night ClO values are somewhat smaller than those from the ChlOE measurements.

We also show in Figure 5 the average ozone mass deficit (in 10<sup>9</sup> kg of ozone relative to the 220 DU value) for September and October of each year. This data was obtained from NASA Ozone Watch ([ozonewatch.gsfc.nasa.gov](http://ozonewatch.gsfc.nasa.gov)) and is based upon data from the Total Ozone Mapping Spectrometer (TOMS) and the Ozone Monitoring Instrument (OMI), with missing data filled in by the Goddard Earth Observing System Model (GEOS-5).



5 **Figure 5 – The climatology plus annual average anomaly (1) day minus night CIO column density for August 28 to September 17 of each year, calculated as described in text. Averages are shown for ChIOE at Scott Base (blue), MLS coincident with Scott Base (solid red) and MLS at the latitude of Scott Base (dashed red line). Also shown is the ozone mass deficit in  $10^9$  kg of ozone relative to the 220 DU value (green line, with right-hand axis). The correlation coefficients between the CIO measurements and the ozone mass deficit are indicated.**

Figure 5 shows a strong correlation between the annual average CIO column and the ozone mass deficit. For the 20 years of ChIOE measurements the correlation coefficient between these is 0.75. The correlation coefficient increases to 0.78 if we do not include 2014, for which there are only 6 ChIOE measurement days out of a possible 21 between August 28 and September 17, as opposed to the annual average of 16.4 measurement days. For the 12 years of Aura MLS CIO column measurements, the correlation coefficient is 0.66 for the measurements coincident with Scott Base, and 0.85 for the zonally averaged measurements at the Scott Base latitude.

#### 4. Temperature and CIO

The fraction of  $Cl_y$  that is in the form of CIO is sensitive to the availability of PSCs, which require low temperatures (below  $\sim 195$ K). As was noted by Santee et al. (2011) for the 2006 winter, the chlorine deactivation and the dissipation of PSCs as observed by the Cloud-Aerosol Lidar and Infrared Pathfinder Satellite Observations (CALIPSO; Pitts et al., 2009) both occur in mid-October. While the variation in CIO measured at any one place and time is

dependent not just upon the local temperature but also upon the temperature history of the measured parcel, we do find that in many cases sudden changes in local temperatures coincide with changes in measured ClO. An example of the sensitivity of ClO to changes in temperature is seen very clearly in Figure 1 of Kremser et al. (2011), where a sudden increase in temperature in early September over Scott Base resulted in a sudden decrease in measured ClO.

Figure 6 shows daily (day minus night) ChlOE column measurements for mid-August to mid-October 2000. This is the same as Figure 3, but for a different (pre-Aura MLS) year. Also shown in Figure 6 are MERRA temperatures at 30 hPa (the pressure level nearest to the ClO mixing ratio peak) within  $\pm 2^\circ$  latitude and  $\pm 15^\circ$  longitude of Scott Base. In addition, we show the climatological temperature from the same 20-year time period as the ChlOE measurements. While the temperatures in late August are clearly colder than those in September, the ClO during this period remains low because of a lack of the sunlight required for the activation of chlorine. Once sunlight becomes available, the ClO column begins to increase and, in this particular year, increases to levels well above the climatology. As Figure 5 shows, this year is second only to 2011 in the annual average ClO column for August 28 to September 17. At the same time, Figure 6 shows that the temperatures are colder than the climatology from August 28 to September 15, and are then warmer than the climatology for 6 of the next 7 days. The date when the temperature crosses from below to above the climatological value is the same date on which the ClO column density crosses from above to below the climatology.

20

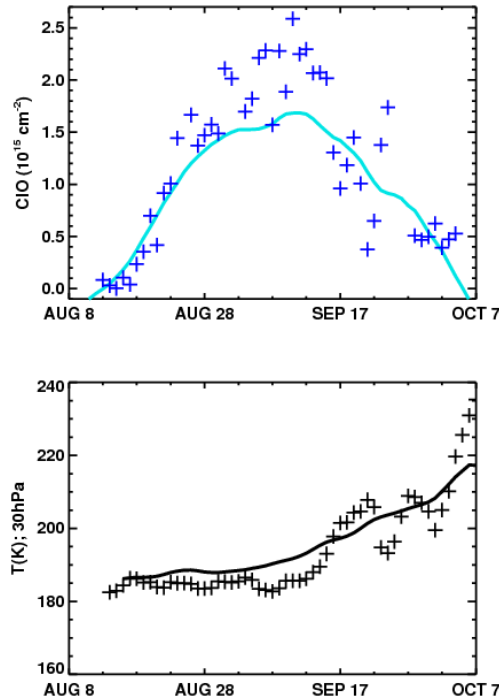


Figure 6 – Top panel: Daily (day minus night) ChIOE1 column density measurements for mid-August to mid-October 2000 (crosses) and a climatology for that period based on the ChIOE measurements from 1996-2015 (solid line). Bottom panel: Daily 30 hPa temperature from MERRA within  $\pm 2^\circ$  latitude and  $\pm 15^\circ$  longitude of Scott Base (crosses) and a 1996-2015 climatology for this location (solid line).

5

The annual average MERRA temperature anomalies at three pressure levels (20, 30, and 40 hPa) are plotted in Figure 7. As in Figure 5, these are calculated by taking the average difference between the daily temperature and the temperature climatology for that day over the 3-week period of August 28 to September 17, but here we do not add back the climatological temperature average. We find that the relationship between temperatures at these three levels changed between 1998 and 1999. The 20 hPa and 30 hPa temperature anomalies suggested extremely cold years from 1996-1998 (at 20 hPa 1996 and 1997 were the coldest years), while at 40 hPa none of these three years was the coldest in the 20-year record.

10

In between the 1998 and 1999 periods that we analyzed, data from the Advanced TIROS (Television Infrared Observation Satellite) Operational Vertical Sounder (ATOVS, on NOAA15) began to be assimilated into the MERRA analysis, and it has been shown that this causes some inhomogeneities in the reanalysis (Pawson, 2012). We therefore compared the MERRA temperatures with sondes launched from Scott Base from 1996-1998, and with sondes launched from 1999-2010. We found that the cold bias of MERRA relative to the sondes at 20 hPa was much reduced in the 1999-2010 MERRA temperatures. Due to the biases in MERRA

20

temperatures indicated by the sonde data, we added 4.0K to the 20 hPa 1996-1998 MERRA temperatures and 2.1K to the 30 hPa temperatures to account for this temperature bias. We also subtracted 0.3K from the 40 hPa 1996-1998 MERRA temperatures. When we estimate chlorine trends in Section 5, it will be particularly important to have temperatures during these first three years of ChLOE measurements that are consistent with temperatures in later years.

Given the anti-correlation between column CIO and temperature, we would expect an anti-correlation between temperature and ozone loss. Just as in Figure 5, we therefore also show in Figure 7 the ozone mass deficit, although in this case with the scale inverted. The magnitude of the anti-correlation between the 30 hPa temperature anomalies over Scott Base and the ozone mass deficit shown in Figure 7 is comparable to that of the correlation between CIO and ozone mass deficit shown in Figure 5, with a correlation coefficient of -0.82, while for the zonal average temperatures the correlation drops to -0.78. The temperature and ozone mass deficit have a slightly weaker correlation at 40 hPa, while at 20 hPa the correlation is slightly stronger for the local temperatures and slightly weaker for the zonal average temperatures.

15

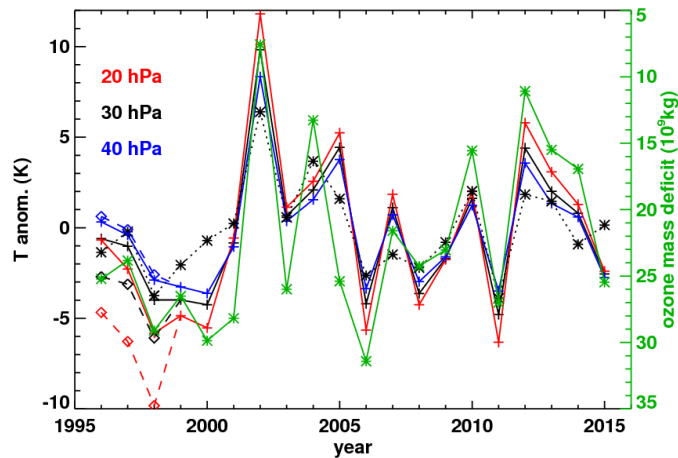


Figure 7 – Annual average temperature anomalies for August 28 to September 17 within  $\pm 2^\circ$  latitude and  $\pm 15^\circ$  longitude of Scott Base. Results are shown at 20 hPa (red), 30 hPa (black), and 40 hPa (blue). The dashed lines for 1996-1998 show the anomalies before applying the bias correction to the MERRA temperatures (see text). Also shown (dotted black line) is the zonal temperature anomaly for this latitude range. The green line shows the ozone mass deficit, with values given on the right-hand axis (as in Figure 5, but with the axis reversed).

Figure 8 presents scatter plots of the annual average column CIO and the 30 hPa temperature anomalies for August 28 to September 17. Since, after the bias correction, the temperature anomalies are very similar for all three pressure levels, the anomalies shown in Figure 8 are nearly independent of the pressure level chosen for the temperatures. We chose 30 hPa since, among the three pressure levels shown in Figure 7, zonally averaged temperatures at

this level showed the highest correlation with MLS zonally averaged column ClO measurements (correlation coefficients of -0.862, -0.863, and -0.781 at 20, 30, and 40 hPa respectively). For the local MLS measurements and ChlOE, the correlation with local temperatures was slightly higher at 20 hPa. Results are shown for ChlOE measurements, as well as for MLS measurements both zonally averaged (with corresponding zonally averaged temperatures) and restricted to within  $\pm 2^\circ$  latitude and  $\pm 15^\circ$  longitude of Scott Base.

To establish a linear fit for the annual average anomalies shown in Figure 8, we need to estimate uncertainties in the temperature and ClO measurements. We estimate these uncertainties by calculating the standard error of the mean for the daily anomalies for each year. This will tend to weight years that have consistently high (or low) ClO column and temperature anomalies, as well as, for ChlOE, years when there are a large number of measurements (MLS almost always has measurements for every day). The uncertainties for each year are generally similar, but in 2014 there were very few ChlOE measurements and these measurements were particularly variable.

15

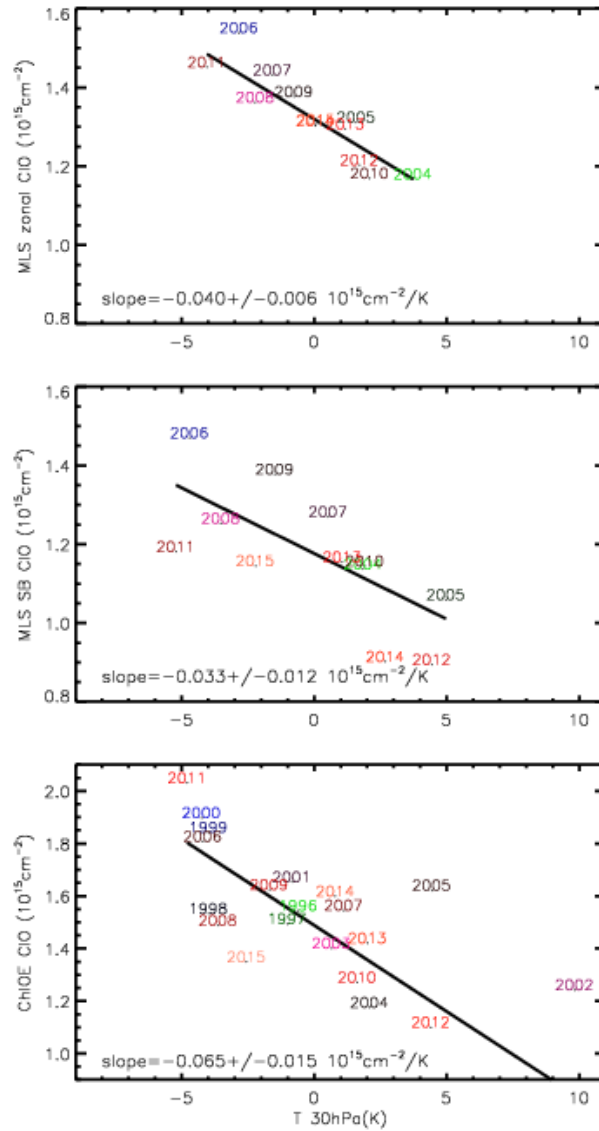


Figure 8 – The climatology plus annual average anomaly for the August 28 to September 17 column CIO (shown in Figure 5) plotted against the temperature anomalies (shown in Figure 7). Also shown are linear fits with a  $1\sigma$  error estimate. Results are shown for the zonally average MLS CIO column measurements and 30 hPa MERRA temperatures within  $\pm 2^\circ$  latitude of Scott Base (top), for MLS CIO and MERRA temperatures with a further restriction to within  $\pm 15^\circ$  longitude of Scott Base (middle), and for ChIOE CIO measurements and MERRA temperatures with this tighter restriction (bottom).

We calculated linear fits and found that the slopes were  $-0.040 \pm 0.006 \text{ } 10^{15} \text{cm}^{-2}/\text{K}$ ,  $-0.033 \pm 0.012 \text{ } 10^{15} \text{cm}^{-2}/\text{K}$ , and  $-0.065 \pm 0.015 \text{ } 10^{15} \text{cm}^{-2}/\text{K}$  for the zonal MLS, Scott Base MLS, and ChIOE CIO measurements, respectively. We attribute the difference in the linear fits between the ChIOE and MLS CIO measurements to the different diurnal sampling of the ChIOE and MLS

measurements. The slopes for the MLS measurements near Scott Base and for the zonally averaged MLS measurements at this latitude are not statistically different.

As a consistency check, we repeated this study using temperatures from the NCEP Reanalysis (REAN2) (Kistler et al., 2001), and calculated fits that were nearly identical to those shown in Figure 8. The slopes were very close to those calculated with MERRA:  $-0.040 \pm 0.006$   $10^{15} \text{cm}^{-2}/\text{K}$ ,  $-0.032 \pm 0.012$   $10^{15} \text{cm}^{-2}/\text{K}$ , and  $-0.068 \pm 0.015$   $10^{15} \text{cm}^{-2}/\text{K}$  for the zonal MLS, Scott Base MLS, and ChlOE ClO measurements, respectively.

## 5. Estimating a Chlorine Trend

There have been a number of studies attempting to quantify the temporal trend in  $\text{Cl}_y$  using measurements of either HCl or ClO. HCl is the primary reservoir species for chlorine, and measurements of HCl in the upper stratosphere show a decline since around 1997 (Anderson et al., 2000; Froidevaux et al. (2006); Jones et al., 2011; Nedoluha et al., 2011). Jones et al. (2011) showed, for a range of latitude bands, a decrease in HCl measured by the Halogen Occultation Experiment (HALOE) of between 0.4 and 0.6%  $\text{yr}^{-1}$  from 1997-2005. Froidevaux et al. (2006) estimated a decrease of  $\sim 0.8 \pm 0.1\%$   $\text{yr}^{-1}$  from Aura MLS HCl measurements over a very brief August 2004 to January 2006 period, but unfortunately the MLS channel measuring HCl near the stratopause experienced rapid deterioration so no extended HCl trend study from the MLS dataset has been possible. Jones et al. (2011) produced a combined ODIN/SMR and MLS ClO dataset for 2001-2008, and calculated a trend of  $-0.7 \pm 0.8\%$   $\text{yr}^{-1}$  ( $2\sigma$ ) in tropical ClO from 35-45km. Nedoluha et al. (2011) used ground-based measurements of ClO from Mauna Kea to show a clear decrease since 1996, and validated the relative consistency of the UARS MLS (1991-1998) and Aura MLS (2004-present) ClO measurements. Finally, Connor et al. (2013) used a reanalyzed version of the ground-based ClO measurements from Mauna Kea and calculated a trend of  $-0.64 \pm 0.15\%$   $\text{yr}^{-1}$  ( $2\sigma$ ) from 1995-2012.

The linear trend in the annual average ChlOE ClO columns from August 28 to September 17 (those shown in Figure 5 from 1996-2015) is  $-1.1 \pm 0.4\%$   $\text{yr}^{-1}$ . However, since the first ChlOE measurement years were colder than average, this trend is almost certainly to some extent the result of increased processing on PSC particles during these years, and is therefore not representative of the trend in  $\text{Cl}_y$ . In addition, interannual variations in dynamics will cause interannual variations in  $\text{Cl}_y$  which will in turn affect the measured ClO. Strahan et al. (2014)



used the compact relationship between nitrous oxide ( $\text{N}_2\text{O}$ ) and  $\text{Cl}_y$ , as established by Schauffler et al. (2003), to estimate the variability in Antarctic  $\text{Cl}_y$  for the years 2004-2012 based upon MLS measurements of  $\text{N}_2\text{O}$ . They found year-to-year variations of  $\text{Cl}_y$  in the vortex on the 500K potential temperature surface of as much as  $\sim 7\%$ .

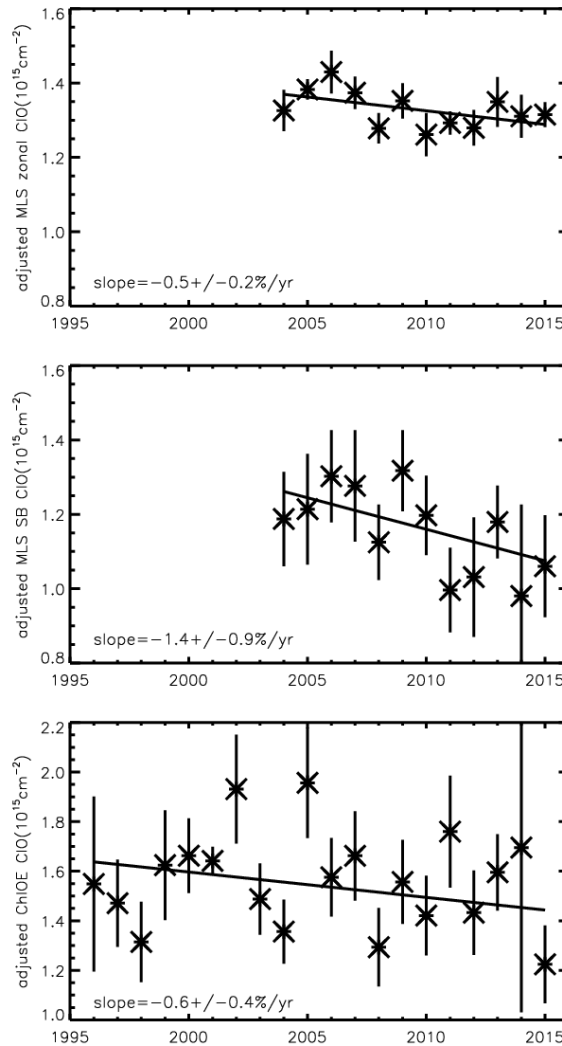
5 Accounting for the dynamical variations over the entire 20-year ChIOE measurement dataset is problematic, and we will not attempt to do so here, but it is certainly possible to account for the interannual temperature variations over this period. Making use of the annual temperature anomalies, we calculate an adjusted annual column CIO, which is given for each year by  $\text{CIO}_{\text{adj}}(\text{year}) = \text{CIO}(\text{year}) - \alpha \Delta T(\text{year})$ , where  $\alpha$  is the temperature dependence of CIO  
10 shown in Figure 8 and  $\Delta T(\text{year})$  is the temperature anomaly for that year. To the extent that we have successfully removed the effect of temperature variations, the variations in the adjusted CIO columns should better represent the variation in  $\text{Cl}_y$ .

The column CIO values, adjusted for interannual temperature variations, are shown in Figure 9. We then calculate a linear trend using these modified column CIO values and express  
15 the trends as a function of the average column values. The resultant trends calculated for zonal MLS, Scott Base MLS (2004-2015), and ChIOE (1996-2015) are  $-0.5 \pm 0.2\% \text{ yr}^{-1}$ ,  $-1.4 \pm 0.9\% \text{ yr}^{-1}$ , and  $-0.6 \pm 0.4\% \text{ yr}^{-1}$ , respectively. Note that the  $1\sigma$  error bars shown in this plot are the same as the error estimates used in establishing the CIO column vs. temperature relationship in Figure 8. The fraction of points falling within  $1\sigma$  of the trend line is approximately what would be  
20 expected given a Gaussian distribution, so our uncertainty estimate seems reasonable. If we use the REAN2 temperatures both to establish the relationship between temperature and CIO column and subsequently to calculate trends then we find trends almost identical to those found with the MERRA temperatures. The calculated trends in adjusted CIO column, as calculated using REAN2 temperatures, are  $-0.6 \pm 0.2\% \text{ yr}^{-1}$ ,  $-1.4 \pm 0.9\% \text{ yr}^{-1}$ , and  $-0.5 \pm 0.4\% \text{ yr}^{-1}$  for zonal MLS,  
25 Scott Base MLS, and ChIOE, respectively.

While the trends are almost insensitive to the choice of temperature dataset, they are somewhat sensitive to the precise choice of dates from which the annual average is determined. Although we believe that we have made an optimal choice for these dates, it is nevertheless instructive to examine this sensitivity. If we add or subtract 5 days from the beginning or end of  
30 the comparison periods and repeat our calculations for these four additional cases we find trends

in adjust ClO columns in the range  $-0.3$  to  $-0.6\%$   $\text{yr}^{-1}$  for the zonal MLS measurements,  $-0.9$  to  $-1.8\%$   $\text{yr}^{-1}$  for the local MLS measurements,  $-0.2$  to  $-0.7\%$   $\text{yr}^{-1}$  for the ChlOE measurements.

Finally, we have also performed the entire analysis using daytime zonal average MLS measurements without subtracting the nighttime measurements. The results are very similar to the results from day minus night measurements, agreeing to within  $1\sigma$  in both the sensitivity of the ClO column to temperature, and in the calculated trend.



10 **Figure 9 – The annual average temperature adjusted ClO columns (see text) for August 28 to September 17. The adjustment is based upon the annual average temperature and the relationship shown in Figure 8 (see text). Results are shown for the zonally averaged MLS measurements within  $\pm 2^\circ$  latitude of Scott Base (top), for MLS measurements within  $\pm 2^\circ$  latitude and  $\pm 15^\circ$  longitude of Scott Base (middle), and for ChlOE measurements at Scott Base (bottom). Also shown is a linear fit to the data. Uncertainties are  $1\sigma$ .**

## 6. Summary

We have shown column ClO from 20 years of ChlOE measurements over Scott Base, Antarctica, as well as from 12 years of Aura MLS measurements near Scott Base and zonally averaged around 78°S. Interannual variations in column ClO over the 3-week period from August 28 to September 17 were correlated with the average ozone mass deficit for September and October ( $r=0.75$  for ChlOE). Such a correlation is to be expected, given that ClO is the catalytic agent in the most important ozone-destroying cycle.

We have also shown that the interannual variation in column ClO is anti-correlated with interannual variations in 30 hPa temperature. This is physically reasonable since colder temperatures increase the availability of polar stratospheric clouds, and these will in turn provide the heterogeneous surfaces for the production of ClO (Molina and Molina, 1987; Solomon, 1999).

The multi-year ChlOE and Aura MLS datasets provided the opportunity to study trends. While there have been a number of studies of trends in Cl<sub>y</sub>, this is to our knowledge the first study that addresses the question of stratospheric Cl<sub>y</sub> trends in the Antarctic region. Since the ozone hole represents the most extreme manifestation of ozone depletion, it is of particular interest to determine whether the trends in Antarctic stratospheric Cl<sub>y</sub>, which underlie the trends in ClO that causes this destruction, are similar to those measured elsewhere.

Because of the strong dependence of ClO on temperature, any calculated trend in ClO could misrepresent the trend in Cl<sub>y</sub>, particularly if there were unusually warm or cold temperatures near the beginning or end of the timeseries. We therefore used the calculated relationship between interannual variations in column ClO and 30 hPa temperature to account for the effect of variations in column ClO caused by changes in temperature. We then calculated trends in temperature-adjusted ClO. The resultant trends for zonal MLS, Scott Base MLS (2004-2015), and ChlOE (1996-2015) were  $-0.5\pm 0.2\%$  yr<sup>-1</sup>,  $-1.4\pm 0.9\%$  yr<sup>-1</sup>, and  $-0.6\pm 0.4\%$  yr<sup>-1</sup>, respectively. While our temperature regression does not account for dynamical effects that might influence ClO trends (e.g. changes in the Brewer-Dobson circulation), these trends are within 1σ of trends in Cl<sub>y</sub> previously found at other latitudes (WMO, 2014). The decrease in ClO is consistent with the trend expected from regulations enacted under the Montreal Protocol.

30

## 7. Acknowledgments

This project was funded by NASA under the Upper Atmosphere Research Program, by the Naval Research Laboratory, and by the Office of Naval Research. We would like to acknowledge the many Antarctica New Zealand Technicians who have supported the daily operation of ChLOE over two decades of measurements. We also acknowledge the logistical support that Antarctica New Zealand has supplied over this period. Work at the Jet Propulsion Laboratory, California Institute of Technology, was carried out under a contract with the National Aeronautics and Space Administration. MLS data are available from the NASA Goddard Earth Science Data Information and Services Center ([acdisc.gsfc.nasa.gov](http://acdisc.gsfc.nasa.gov)). Sonde temperature data were collected under support from the National Science Foundation.

## 8. References

- Anderson, J., Russell III, J. M., Solomon, S., and Deaver, L. E. (2000), Halogen Occultation Experiment confirmation of stratospheric chlorine decreases in accordance with the Montreal Protocol, *J. Geophys. Res.*, 105, 4483–4490, 2000.
- Connor, B. J., T. Mooney, J. Barrett, P. Solomon, A. Parrish, and M. Santee (2007), Comparison of ClO measurements from the Aura Microwave Limb Sounder to ground-based microwave measurements at Scott Base, Antarctica, in spring 2005, *J. Geophys. Res.*, 112, D24S42, doi:10.1029/2007JD008792.
- Connor, B. J., T. Mooney, G. E. Nedoluha, J. W. Barrett, A. Parrish, J. Koda, M. L. Santee, and R. M. Gomez (2013), Re-analysis of ground-based microwave ClO measurements from Mauna Kea, 1992 to early 2012, *Atmos. Chem. Phys.*, 13, 8643–8650, 2013.
- de Zafra, R. L., M. Jaramillo, A. Parrish, P. Solomon, B. Connor, and J. Barrett (1987), High concentrations of chlorine monoxide at low altitudes in the Antarctic spring stratosphere: Diurnal variation, *Nature*, 328, 408–411.
- Froidevaux, L., et al. (2006), Temporal decrease in upper atmospheric chlorine, *Geophys. Res. Lett.*, 33, L23812, doi:10.1029/2006GL027600.
- Jones, A., et al. (2011), Analysis of HCl and ClO time series in the upper stratosphere using satellite data sets, *Atmos. Chem. Phys.*, 11, 5321–5333, 2011.
- Kistler, R., et al. (2001), The NCEP-NCAR 50-year reanalysis: Monthly means CDROM and documentation, *Bull. Am. Meteorol. Soc.*, 82, 247–267.

- Kremser, S., R. Schofield, G. E. Bodeker, B. J. Connor, M. Rex, J. Barrett, T. Mooney, R. J. Salawitch, T. Canty, K. Frieler, M. P. Chipperfield, U. Langematz, and W. Feng (2011), Retrievals of chlorine chemistry kinetic parameters from Antarctic ClO microwave radiometer measurements, *Atmos. Chem. Phys.*, 11, 5183–5193, 2011.
- 5 Livesey, N. J., et al. (2015), Version 4.2x Level 2 data quality and description document, Tech. Rep. JPL D-33509 Rev. A, Jet Propulsion Laboratory, available from <http://mls.jpl.nasa.gov>.
- Molina, L. T. and Molina, M. J. (1987), Production of Cl<sub>2</sub>O<sub>2</sub> from the self-reaction of the ClO radical, *J. Phys. Chem.*, 91, 433–436, doi:10.1021/j100286a035, 1987.
- 10 Nedoluha, G. E., et al. (2011), Ground-based measurements of ClO from Mauna Kea and intercomparisons with Aura and UARS MLS, *J. Geophys. Res.*, 116, D02307, doi:10.1029/2010JD014732.
- Parrish, A., R. L. de Zafra, P. M. Solomon, J. W. Barrett, and E. R. Carlson (1981), Chlorine Oxide in the Stratospheric Ozone Layer: Ground-Based Detection and Measurements, *Science*, 211, 1158-1160, 1981.
- 15 Pawson, S.: Representation of the Middle-to-Upper Stratosphere in MERRA, Global Modeling and Assimilation Office Annual Report & Research Highlights, 42–43, 2012.
- Pitts, M. C., L. R. Poole, and L. W. Thomason (2009), CALIPSO polar stratospheric cloud observations: second-generation detection algorithm and composition discrimination, *Atmos. Chem. Phys.*, 9, 7577–7589.
- 20 Rienecker, M. M., et al. (2011), MERRA: NASA’s Modern Era Retrospective Analysis for Research and Applications, *J. Clim.*, 24, 3624–3648.
- Rodgers, C. D. (2000), *Inverse Methods for Atmospheric Sounding*, World Scientific Publishing Co., Hackensack, NJ.
- 25 Salawitch, R. J., et al. (1993), Chemical loss of ozone in the Arctic polar vortex in the winter of 1991-1992, *Science*, 261, 1146-1149.
- Santee, M. L., G. L. Manney, N. J. Livesey, L. Froidevaux, I. A. MacKenzie, H. C. Pumphrey, W. G. Read, M. J. Schwartz, J. W. Waters, and R. S. Harwood (2005), Polar processing and development of the 2004 Antarctic ozone hole: First results from MLS on Aura, *Geophys. Res. Lett.*, 32, L12817, doi:10.1029/2005GL022582.
- 30

- Santee, M. L., et al. (2008), Validation of the Aura Microwave Limb Sounder ClO measurements, *J. Geophys. Res.*, 113, D15S22, doi:10.1029/2007JD008762.
- Santee, M. L., G. L. Manney, N. J. Livesey, L. Froidevaux, M. J. Schwartz, and W. G. Read (2011), Trace gas evolution in the lowermost stratosphere from Aura Microwave Limb Sounder measurements, *J. Geophys. Res.*, 116, D18306, doi:10.1029/2011JD015590.
- Schauffler, S. M., E. L. Atlas, S. G. Donnelly, A. Andrews, S. A. Montzka, J. W. Elkins, D. F. Hurst, P. A. Romashkin, G. S. Dutton, and V. Stroud (2003), Chlorine budget and partitioning during the Stratospheric Aerosol and Gas Experiment (SAGE) III Ozone Loss and Validation Experiment (SOLVE), *J. Geophys. Res.*, 108(D5), 4173, doi:10.1029/2001JD002040.
- Solomon, P. M., B. Connor, R. L. de Zafra, A. Parrish, J. Barrett, and M. Jaramillo (1987), High concentrations of chlorine monoxide at low altitudes in the Antarctic spring stratosphere: Secular variation, *Nature*, 328, 411-413.
- Solomon, P., J. Barrett, B.J. Connor, S. Zoonematkermani, A. Parrish, A.M. Lee, J.A. Pyle, and M.P. Chipperfield (2000), Seasonal observations of chlorine monoxide in the stratosphere over Antarctica during the 1996-1998 ozone holes and comparison with the SLIMCAT 3D model, *J. Geophys. Res.*, 105 (D23), 28979-29001.
- Solomon, P., B. Connor, J. Barrett, T. Mooney, A. Lee, and A. Parrish (2002), Measurements of stratospheric ClO over Antarctica in 1996-2000 and implications for ClO dimer chemistry, *Geophys. Res. Lett.*, 29 (15), 10.1029/2002GL015232, 2002.
- Solomon, S. (1999), Stratospheric ozone depletion, A review of concepts and history, *Rev. Geophys.*, 37, 275–316, 1999.
- Strahan, S. E., A. R. Douglass, P. A. Newman, and S. D. Steenrod (2014), Inorganic chlorine variability in the Antarctic vortex and implications for ozone recovery, *J. Geophys. Res. Atmos.*, 119, 14,098–14,109, doi:10.1002/2014JD022295.
- Waters, J.W., L. Froidevaux, W.G. Read, G.L. Manney, L.S. Elson, D.A. Flower, R.F. Jarnot, and R.S. Harwood (1993), Stratospheric ClO and ozone from the Microwave Limb Sounder on the Upper Atmospheric Research Satellite, *Nature*, 362, 597-602.
- WMO (World Meteorological Organization), Scientific Assessment of Ozone Depletion: 2014, World Meteorological Organization, Global Ozone Research and Monitoring Project- Report No. 55, 416 pp., Geneva, Switzerland, 2014.

